# CFD ANALYSIS AND FLOW MODEL REDUCTION FOR SURFACTANT PRODUCTION IN HELIX REACTOR

N.M. Nikačević<sup>1,3\*</sup>, L. Thielen<sup>2,4</sup>, A. Twerda<sup>2</sup>, P.M.J Van den Hof<sup>1</sup>

<sup>1</sup> Eindhoven University of Technology, Den Dolech 2, 5612 AZ Eindhoven, The Netherlands

<sup>2</sup> TNO Science, P.O. Box 155 NL-2600 AD Delft, The Netherlands

<sup>3</sup> University of Belgrade, Faculty of Technology and Metallurgy, Karnegijeva 4, 11000 Beograd, Serbia

<sup>4</sup> CelSian Glass & Solar B.V., P.O. Box 7051, 5605 JB Eindhoven, The Netherlands

Received 10.10.2013.

Revised 9.1.2014.

Accepted 6.2.2014.

<sup>\*</sup> Corresponding author, email: <a href="mailto:nikacevic@tmf.bg.ac.rs">nikacevic@tmf.bg.ac.rs</a>, phone: +381113303652, fax: +381113370387

#### **Abstract**

Flow pattern analysis in a spiral Helix reactor is conducted, for the application in the commercial surfactant production. Step change response curves (SCR) were obtained from numerical tracer experiments by three-dimensional computational fluid dynamics (CFD) simulations. Non-reactive flow is simulated, though viscosity is treated as variable in the direction of flow, as it increases during the reaction. The design and operating parameters (reactor diameter, number of coils and inlet velocity) are varied in CFD simulations, in order to examine the effects on the flow pattern. Given that 3D simulations are not practical for fast computations needed for optimization, scale-up and control, CFD flow model is reduced to one-dimensional axial dispersion (AD) model with spatially variable dispersion coefficient. Dimensionless dispersion coefficient (Pe) is estimated under different conditions and results are analyzed. Finally, correlation which relates Pe number with Reynolds number and number of coils from the reactor entrance is proposed for the particular reactor application and conditions.

**Keywords**: CFD simulation, Flow pattern analysis, axial dispersion model, process intensification, batch to continuous

# **Highlights:**

- Helix reactor is suitable for slow reactions in surfactants production due to good flow pattern
- Secondary flow (Dean vortices) in Helix occur in laminar regime with Re even less than 100
- Axial dispersion model represents surfactant laminar flow in Helix better than pure convective one
- Number of Helix coils strongly affects the development of (secondary) flow pattern
- Peclet number is considered variable to account for viscosity change and number of coils effect

#### 1. Introduction

Fine chemicals and pharmaceuticals are still dominantly produced in batch operated stirred-tank reactors. However, global market competition, increase in energy and other production costs, demands for high quality products and reduction of waste are forcing pharmaceutical, fine chemicals and biochemical industries, to search for radical solutions [1-3]. One of the most effective ways to improve the overall production is transition from batch to continuous processes. Intensified continuous reactors, e.g. micro/milli-reactors, oscillatory flow, static mixer etc., radically improve mixing properties and thus allow a reaction to approach its intrinsic kinetic limits. This directly relates to improved productivity and selectivity and reduction in energy consumption and waste generation [3-5].

The case of interest is production of the commercial surfactant, for which continuous operation is considered and investigated. The reaction is relatively slow, thus classical continuous tubular reactors would be impractically long for flow regimes which provide sufficient heat transfer and time distribution. the narrow residence Furthermore. commercial manufacturing of the particular surfactant requires large capacities, thus microreactors are not suitable due to their size and numbering-up issues. Therefore, the selected reactor is TNO Helix, which is designed as a helicoidal tube (Figure 1). This type of reactor enables very good radial mixing of fluid, due to the presence of so-called secondary flow - Dean vortices in a spiral tube, as illustrated in Figure 1 [6,7]. In the Helix, plug flow is approached with low Re numbers which correspond to laminar regime in a straight tube. The Dean vortices enhance mixing enabling high mass and heat transfer rates [6,7]. Further, the Helix's compact design and the use of moderate diameters (cm scale) could provide sufficient capacities, making it potentially suitable for industrial-scale production.

## Figure 1.

However, in the case of particular surfactant production, relatively low Re numbers are to be applied (lower then 100), since necessary residence times are quite long, and viscosity is rather high. Furthermore, viscosity increases during the reaction, thus Re number is decreasing. Moreover, for moderately low number of Helix coils, which could be expected for this application, desired flow pattern may not be fully developed. For the reasons listed, flow pattern in Helix is complex and may deviate from plug flow, which is investigated in this work via detailed numerical computational fluid dynamics (CFD) simulations. Given that 3D simulations are not practical for fast computations needed for optimization, scale-up and control, the goal of this work is to reduce CFD flow model to one-dimensional axial dispersion (AD) model with spatially variable dispersion coefficient.

### 1. Numerical experiments – CFD simulations of Helix reactor

The objective is to investigate the flow of moderately viscous fluid in spiral Helix and to examine the influence of fluid velocity, tube diameter and number of coils on the radial and axial mixing. For this purpose, three-dimensional CFD simulations of surfactant flow in Helix have been performed. It is anticipated that radial mixing is excellent, due to the presence of secondary flow and Dean vortices [6,7]. Therefore, the focus is on axial mixing and CFD simulation results are used to extract step change response curves (SCR). These numerically obtained SCR curves are the base for the CFD model reduction to one-dimensional AD model and derivation of Peclet (Pe) numbers – dimensionless axial dispersion coefficients. Further, the influences of flow conditions (velocity) and reactor geometry (diameter and number of coils) are analyzed. Finally, an empirical correlation that relates Pe numbers with Re and number of coils is offered, which could be used for one-dimensional modeling of surfactant production in Helix reactor.

Kinetic viscosity of the reaction mixture for the surfactant production increases as the reaction propagates, starting from around 0.008 Pas and ending at 0.03-0.042 Pas. Obviously, liquid viscosity decreases with the increase of temperature. The change of viscosity along the reactor due to reaction propagation is taken into account in the CFD model, through an

empirical correlation. The dependence of viscosity on reactant conversion and temperature is investigated experimentally. The apparent viscosity of the reaction mixture was measured using Brookfiled LVT viscometer in a stirred tank operating at 30 or 60 RPM. Viscosity was measured at different reaction conversions, from 0% to 100%, and different temperatures, from 22 to 70 °C. The Arrhenius type empirical correlation was set:

$$\mu(Z,T) = \mu_0 \cdot \exp\left(a \cdot Z + \frac{E}{RT}\right) \tag{1}$$

where Z is reactant conversion, R is gas constant and T is temperature. Experimental results have been used for the estimation of parameters in gPROMS and resulting values are:

$$\mu_0 = 1 \, mPas$$
,  $a = 1.51 \, E = 5229 \, J / mol$ 

Correlation is validated by the comparison of calculated and measured viscosities under given experimental conditions. The agreement is fairly good, with the average relative error of 9.8% and standard deviation ranging from 0.001 to 0.007. Estimation results passed optimization tests – fit test with weighted residual and correlation matrix. The results show that predicted viscosity is slightly overestimated, especially for higher temperatures. Nevertheless, it can be used with acceptable confidence for the simulation of the particular flow in the Helix.

The reaction kinetics is not included in the CFD model. Nevertheless it is assumed that viscosity is changing along the reactor as in eq. (1) and that it reaches the value which corresponds to 100% conversion at the end of the reactor (no matter how long it is). This assumption implies that the reactant conversion is changing linearly along the reactor length and thus at the end of the reactor, a full conversion is achieved (Z equals to the dimensionless position along the reactor  $\xi$ ). This is rather rough approximation for the reaction propagation, but for viscosity it gives acceptably good physical picture. Further, CFD flow analyses are carried out at isothermal conditions and physical properties at 50°C are used (density is 989.3 kg/m³). Figure 2

shows 3D Helix geometry model and how viscosity changes along the reactors with 3 and 12 coils (windings).

CFD model is computed using CelSian's software package X-stream, with a solver based on finite volume element method, solving Navier-Stokes equations in laminar regime [details in the ref. 8, 9]. The grids in X-stream are 3D multi-block structured, body-fitted, and the code is fully parallelized [8]. The 3D geometry and mesh is constructed in Gambit, with a dense mesh consisting of 230,000 cells per winding (coil). TNO Helix standard geometry ratios, between tube diameter, coil diameter and coil pitch, have been used [6]. The current model, geometry and mesh are formulated on the basis of a previously developed Helix models [9,10]. Overall 11 numerical experiments are performed. In order to study the influence of the parameters on the flow pattern, different inlet velocities, tube diameters and number of coils are used, according to the Table 1. Table 1 also presents inlet and outlet Re numbers which correspond to the chosen velocity, diameter and viscosity (calculated using eq. (1). The conditions have been selected to cover ranges of Re numbers and reactor lengths which provide sufficient residence time needed for the surfactant production. Furthermore, in the tubes of different diameters flow similarity is kept (same Re number profiles), which would be a reasonable scale-up strategy.

### Figure 2., Table 1.

As mentioned above the goal is to obtain step change response curves out of the CFD simulations. Thus, numerical dynamic tracer experiments are performed with a step change in concentration of the "tracer" (from 0 to 1) at the inlet. Obviously, the "tracer" has identical physical properties as the "basic" fluid, for which stationary flow simulation was done before the introduction of the tracer (initial conditions). After the step change, concentration of the tracer is registered in time at the reactor exit, for each experiment. Figure 3 presents selected cross-section profiles of tracer concentrations at the exit, at the theoretical mean residence times of the tracer ( $=L/U_{av}$ ).

Concentration fields in Figure 3, as assumed, confirm existence of the secondary flow, visible in the graph, even with low Re numbers and laminar flow conditions. Comparison of Figures 3 a) and b) show that higher inlet velocities (higher Re) create secondary flow (Dean vortices) more intensively, as it may be expected. Figure 3 c) demonstrates that a high number of coils (12) provides much more homogeneous concentration field than the Helix with 3 coils (Fig. 3 b). Thus total number of coils in Helix appears to be an important factor. Concentration fields in Figure 3 d) and e) are almost identical, which proofs that a coil diameter does not influence the mixing, if the same Re profiles are applied at different scales. Comparison of subplots f) and e) confirms that higher number of coils (6 against 3, for the same flow conditions and diameters) provide more effective radial mixing.

As the objective of the work is to offer one-dimensional flow model, further analysis concentrates on axial dispersion, which would lump the non-ideality of the flow. Therefore, SCR curves (F curves), as the responses on step change at input, are obtained at the exit, for each experiment. F curves are also gathered at more axial positions through the reactor (every half of a coil, after a first coil) in order to get more information. F curves are obtained by spatial cross-section averaging of the tracer fraction at a certain point. Figure 4 a) and b) present F curves obtained from CFD simulations for all 11 experiments, at the outlet of the reactors. S-shape curves presented in Figure 4 confirm that there is considerable axial mixing, and that axially dispersed plug flow model could be suitable for the flow model reduction.

Figure 4.

# 2. CFD model reduction to AD model with variable dispersion coefficient

Numerically obtained (CFD) F curves have been used for estimation of axial dispersion coefficient (D) and corresponding dimensionless mixing

number – Peclet (Pe) number for axially dispersion plug flow model. Higher the Pe number, less axial mixing is present and flow approaches the ideal plug flow pattern. Further on, the influences of flow conditions and reactor design characteristics on estimated Pe numbers are analyzed. As demonstrated earlier, spiral design of tubes facilitate plug flow pattern behavior. However, for relatively small number of coils and low velocities characteristic for this study, it is anticipated that axial dispersion is decreasing along the tube as the fluid passes through the coils. Further, viscosity is increasing along the reactor, thus Pe number is considered to be axially variable.

Dynamic material balance for a tracer has been set and Pe numbers are estimated at different positions, for different experimental conditions. For any given experiment j characterized by a superficial fluid velocity  $(u_{av})$ , given measurement point k characterized by a certain length from the reactor inlet  $(L_k)$ , the tracer material balance is:

$$\frac{\partial X_{j,k}}{\partial t} = -\frac{u_{av,j}}{L_k} \frac{\partial X_{j,k}}{\partial \xi} + \frac{D_{j,k}}{L_k^2} \frac{\partial X_{j,k}}{\partial \xi}$$
(2)

$$Pe_{j,k} = \frac{u_{av,j} \cdot L_k}{D_{j,k}} \tag{3}$$

For the axial dispersion model, Danckwerts' boundary conditions are applied. For step change at reactor inlet, the condition is:

$$X_{j,k,in} = 1 + \frac{D_{j,k}}{u_{av,j}L_k} \frac{\partial X_{j,k,in}}{\partial \xi}$$
(4)

For the reactor exit, the boundary condition is:

$$\frac{\partial X_{j,k,out}}{\partial \mathcal{E}} = 0 \tag{5}$$

The axial dispersion coefficient (eq. 2) and subsequent Pe number (eq. 3) are estimated after the inlet zone, where the flow pattern is still not developed to be represented by plug flow with axial dispersion. This inlet zone

spreads to the end of the first coil. Parameter estimations are done in gPROMS software, using specific toolbox for parameter estimation (dynamic optimization program). Overall, 78 Pe numbers have been estimated from 11 experiments, under the conditions given in Table 1. All estimations have passed necessary optimization tests (fit test with weighted residual, t-value confidence test, variance-covariance matrix) and the standard deviations were in the range from 0.62 to 0.9.

Results – estimated Pe numbers are presented in Figures 5 a-d). In Figure 5 a), Pe numbers are plotted against Re numbers for the first five experiments, with the same diameter (16 mm) and total length of 3 coils. The lines connect Pe numbers at different positions along the reactor – after 1 coil, after 1.5 and so on. It is visible that Pe number slightly increases with the increase of Re number. To reiterate, Re numbers are decreasing along the reactor due to the increase of viscosity. Figure 5 a) also shows that the distance from the inlet has more effects on Pe number than Re number. This is more evident in Figure 5 b) where Pe numbers for three experiments with the same inlet velocity (10 mm/s), and diameter, but different total number of coils are presented. It is visible from Figure 5 b) that Pe number increases down the reactor, even though Re number is decreasing. It should be noted that the reactor inlet correspond to higher Re numbers (right hand side of the plot).

The influence of the axial position from the inlet and number of coils on Pe number is also displayed in Figure 5 c). In this figure, line connects experiment with the same velocity. All of them presented have the same reactor diameter (16 mm). Figure 5 c) demonstrate sharp rise of Pe number with the increase in the number of coils – positions from the inlet. Almost all experiments follow the same trend. Only the results for experiment 9 deviate significantly and Pe numbers were unexpectedly high. Since these Pe numbers fall far out of the region of the other experimental values they were not considered for deriving Pe number empirical correlation.

The influence of reactor diameter can be analyzed with plots in Figure 5 d). Figure 5 d) display Pe numbers vs. position along the reactors of different diameters (5, 16 and 50 mm) and two total number of coils (3 and 6). The inlet velocities in different-sized reactors are set to give the same Re profile in reactors (flow similarity). It can be seen that a diameter has modest influence, if the same Re number profile is applied at different scales. This figure also demonstrates that the influence of the position from the inlet diameter is the most significant factor. Therefore, a reactor diameter will not be included in the Pe number correlation directly, as it has a minor influence. Obviously it is included in Re number, thus appearing indirectly.

Presented analysis results in a dimensionless "empirical" correlation for Pe number, which is variable along the reactor position ( $\xi$ ). It relates Pe number with axially variable Re number and number of coils from the inlet. A non-linear regression was performed in MATLAB and resulting correlation is:

$$Pe(\xi) = 6.42 \cdot \text{Re}(\xi)^{0.07} N(\xi)^{0.45}$$
 (6)

The number of coil, N is related with a position, for a standard design of Helix reactor, as:

$$N(\xi) = \frac{\xi \cdot L}{12\pi \cdot d} \tag{7}$$

where d is reactor diameter and L is reactor overall length. Reynolds number is calculated as usual:

$$\operatorname{Re}(\xi) = \frac{\rho \cdot u_{av} \cdot d}{\mu(\xi)} \tag{8}$$

where  $\rho$  is the average density, and viscosity depends on axial position (conversion) as defined in eq. (1). The correlation holds for the following range of variables 3 < Re < 80, 1 < N <12 and 5 < d < 50 mm. In an overall reactor model, *Pe* number for a first coil needs to be calculated as well. Therefore, for the first coil, the equation (6) is reduced to:

The correlation has R<sup>2</sup> value of 0.97, average relative error of around 7% and standard deviation of 4.2 and it is also validated by simulations. The flow through Helix was simulated using AD model defined in eqs. (2-5) with variable Pe number, calculated by eqs. (6) and (9) under particular experimental conditions. The resulting F curves were then compared with experimental CFD curves. Moreover, additional F curves were calculated using a pure convective laminar flow model (CON) in order to compare models and to justify the choice of the axial dispersion model. The pure convective model would be suitable for the particular surfactant flow in a straight tube, as the viscosity is considerably high, molecular diffusion coefficient is rather low and Re numbers are in laminar regime [11]. However, presence of secondary flow in Helix ensures good radial mixing and thus the following analysis demonstrates that convective flow model is less accurate than AD model. The simple equations for F curve calculation according to CON model can be found in ref. [11].

Selected results for RTD curves are presented in Figures 6 a-c). Figure 6 a) shows comparison of F curves for three experiments performed in the same sized reactor (d=16 mm, N=3). So called experimental curves (numerical CFD 3D) are potted with dashed line and labeled as 3D. The agreement between experimental curves and simulated curves using Pe correlation and AD model (solid lines, labeled as AD) is good for all experiments. Convective laminar flow model was presented for experiment 1 (dashed-point line, labeled CON). It can be seen that AD model predicts flow pattern better, especially after the initial period. At the beginning of RTD curve, AD model predicts more axial mixing then it was obtained through rigorous CFD simulation. In this region convective flow model fits better, however after that it considerably deviates from CFD curve.

## Figure 6.

Similar trends are demonstrated in Figure 6 b), where the results for three experiments are presented. Again 16 mm dia. reactor is simulated, with the same inlet velocity, but different lengths (number of coils: 3, 6, 12). Figure 10 demonstrates that agreement between AD model simulations and rigorous 3D model simulations is acceptably good. The discrepancy increases for the longer reactors, with more coils, where reduced AD model predicts more axial mixing than 3D model. This is a conservative result and as such can be accepted for the overall reactor modeling, especially as the discrepancy for the CON model is much higher, as it can be seen in Figure 6 b).

Good agreement between reduced AD model and full 3D simulations are demonstrated for larger size Helix in Figure 6 c). Again, the agreement is decreasing for the larger number of coils. In conclusion, this graph proofs that the correlation (6) can be used for a prediction of a flow pattern in different sized Helix reactors (within investigated diameters), which is important information for a scale-up.

#### **Conclusions**

Helix reactor could be suitable for slow reactions, characteristic for fine chemical and pharmaceutical industries, as it exhibits good radial mixing with low superficial velocities which correspond to laminar regime. In the case of surfactant production, with changeable viscosity during the reaction and low Reynolds numbers, CFD simulations of Helix demonstrated that there is still a considerable axial mixing. Detailed CFD model was approximated with one-dimensional axial dispersion (AD) model, with spatially variable Peclet number. Pe numbers, estimated from CFD results, depend significantly on the number of the coils from the entrance (N) and slightly on Re number. The first effect is caused by the slow formation of Dean vortices as the fluid passes through the coils. A correlation for Pe dependence on Re and N is proposed (holds for N < 12 and Re < 100). The investigation showed that, if Re profiles are kept constant at different scales (diameters 5-50 mm), the flow pattern would stay the same, which is important fact for scale-up. The correlation is verified by the comparison with CFD obtained F curves. The comparative

analysis confirmed that AD model outperforms a pure convective flow model, which is suitable for surfactant flow in straight pipes.

## **Acknowledgements**

The authors acknowledge Christopher Jones and Linda Pellens from Procter and Gamble for providing results from viscosity measurements. This work is a part of the ISPT project CORIAC.

### **Nomenclature**

```
a - coefficient for viscosity dependence on reactant conversion, (-), eq. (1)
```

```
D - axial dispersion coefficient, (m<sup>2</sup>/s)
```

```
d - reactor diameter, (m)
```

E - coefficient for viscosity dependence on temperature, (J/mol), eq. (1)

*F* - step change response curve, fraction of a tracer at the output

L - reactor length, (m)

Pe - dimensionless axial dispersion coefficient, Peclet number, (-), eq. (3)

R - universal gas constant, (J/molK)

Re - Reynolds number, (-), eq. (8)

T - temperature, (K)

*t* - time, (s)

 $u_{av}$  - average superficial velocity, (m/s)

X - tracer dimensionless concentration, tracer fraction, (-)

```
Z - reactant conversion, (-)
```

# **Greek letters**

```
\mu - dynamic viscosity, (Pas) \mu_0 = \text{dynamic viscosity at 293K and zero conversion, (Pas), eq. (1)} \rho = \text{density, (kg/m}^3) \xi = \text{dimensionless position, (-)}
```

# Subscripts

```
j - experiment j, conditions given in Table 1
```

k - measurement k at different positions along the Helix reactor

in - inlet

out -outlet

#### References

- [1] E. H. Stitt, Chem. Eng. J. 90(1-2) (2002) 47-60
- [2] P. Poechlauer, J. Manley, R. Broxterman, B. Gregertsen, M. Ridemark, Org. Process Res. Dev., 16(10) (2012), 1586-1590
- [3] M. P. Dudukovic, Science 325 (2009) 698-701
- [4] V. Hessel, S. Hardt, H. Lowe, Chemical Micro Process Engineering. Fundamentals, Modeling and Reactions, Wiley-VCH, New York (2004)
- [5] N. M. Nikačević, A. E. M. Huesman, P.M.J. Van den Hof, A. I. Stankiewicz, Chem. Eng. Process 52 (2012) 1-15
- [6] TNO The Netherlands, Patent No. WO2009151322 (A1) (2009)
- [7] P. Geerdink, A. Van De Runstraat, E. L. V. Goetheer, C. P. M. Roelands, In Proceedings of AIChE Annual Meeting, Nashville, USA (2009)
- [8] P. Ferziger, M. Perić, Computational Methods for Fluid Dynamics, 3rd ed., Springer, Berlin (2002)
- [9] L. Thielen, A. M. Lankhorst, B. D. Paarhuis, In proceedings of NAFEMS World Congress, Vancouver, Canada (2007)
- [10] A. M.Lankhorst, B. D. Paarhuis, H. J. C. M. Terhorst, P. J. P. M. Simons,C. R. Kleijn, Surf. Coatings Techn. 201 (2007) 8842.
- [11] O. Levenspiel, The Chemical Reactor Omnibook, OSU, Corvallis (1993)

Table 1. Conditions for CFD 3D simulations of the flow pattern in Helix reactor

No.	Diameter	No. of coils	Inlet	Inlet Re	Outlet
exp.	[mm]		velocity,		Re
			u <sub>av</sub> [mm/s]		
1.	16	3	5	13.5	3.0
2.	16	3	7.5	20.2	4.4
3.	16	3	10	27.0	5.9
4.	16	3	15	40.5	8.9
5.	16	3	30	81.0	17.7
6.	5	3	31.4	27.0	5.9
7.	50	3	3.1	27.0	5.9
8.	16	6	10	27.0	5.9
9.	16	9	5	13.5	3.0
10.	16	12	10	27.0	5.9
11.	50	6	3.1	27.0	5.9



Figure 1. TNO Helix reactor. Typical construction and an illustration of the secondary flow (Dean vortices) inside the helicoidal tube (Adapted from ref. [7] with a permission.)

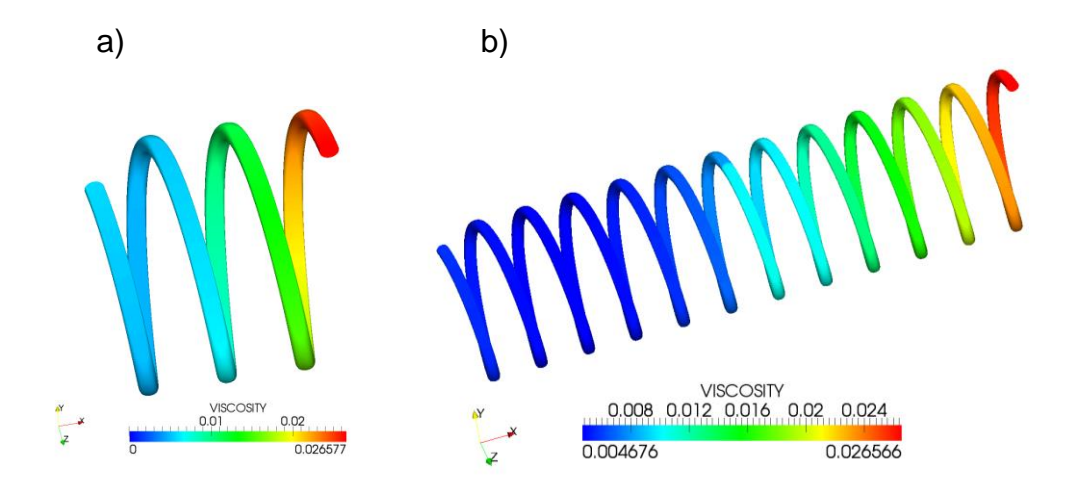


Figure 2. Viscosity profile for the surfactant production in Helix with: a) 3 coils, b) 12 coils

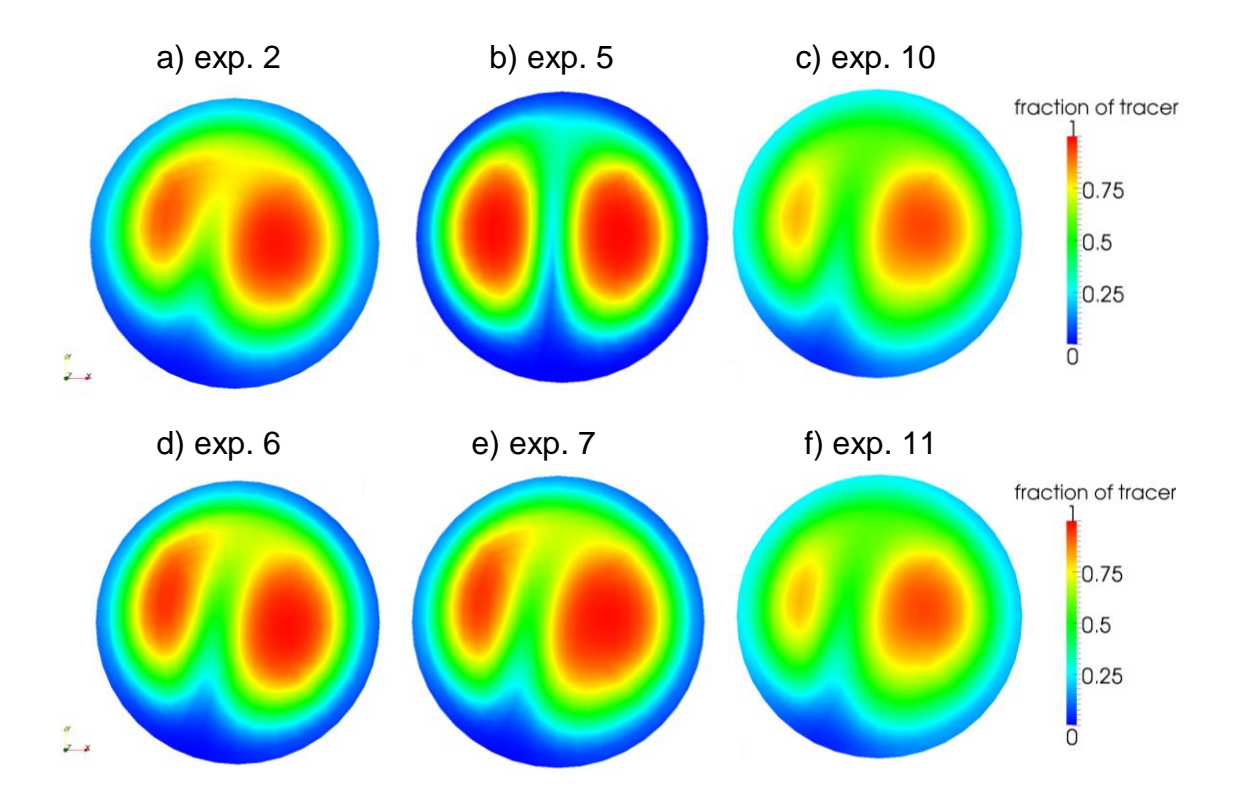


Figure 3. Tracer concentration profiles at the Helix exit at the theoretical mean residence times. a) experiment 2, b) experiment 5, c) experiment 10, d) experiment 6, e) experiment 7, f) experiment 11 (conditions given in Table 1).

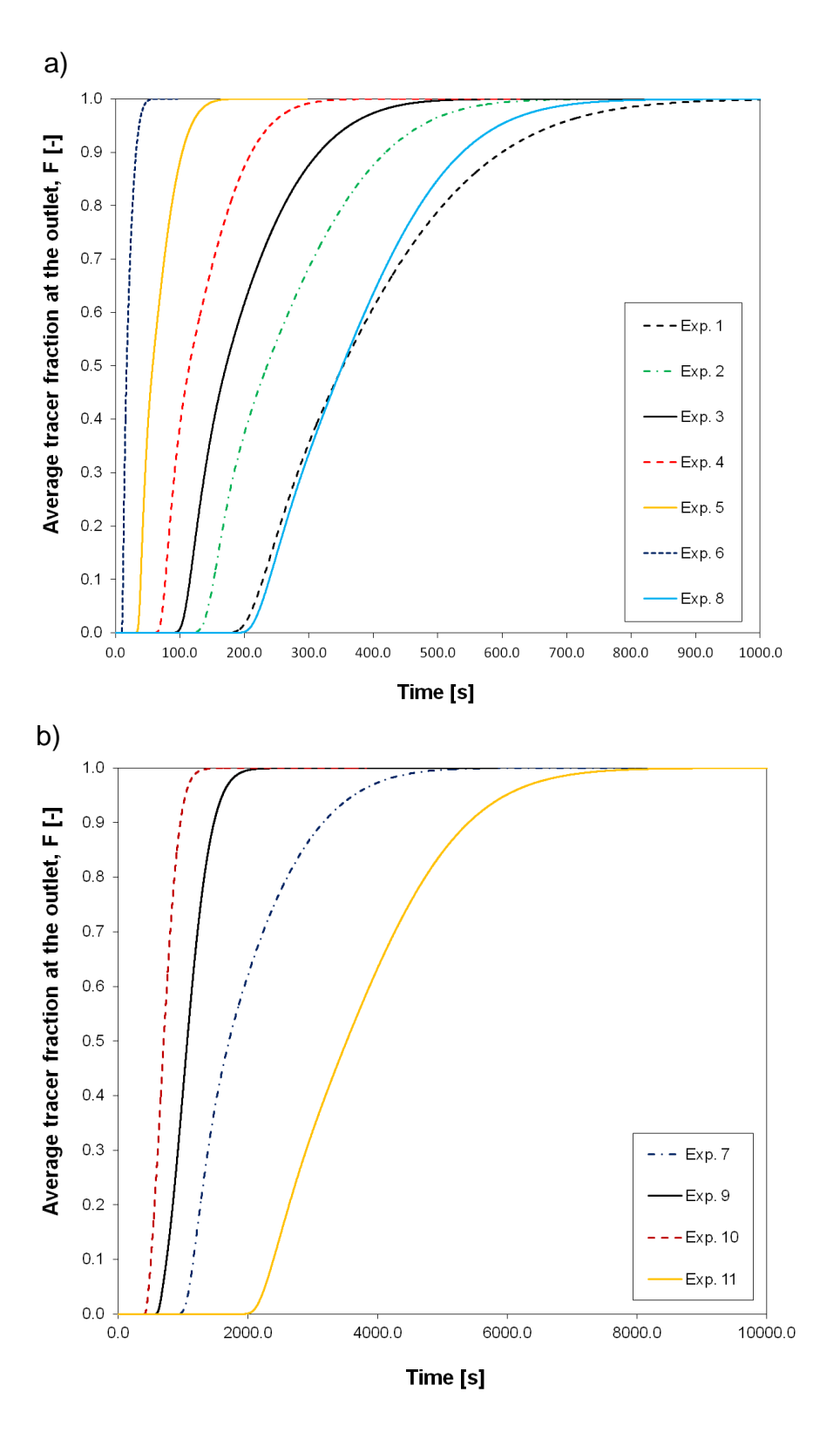


Figure 4. Step change response curves (F) for Helix reactor obtained from CFD 3D simulations, under different conditions presented in Table 1: a) experiments 1-6,8 b) experiments 7,9-11

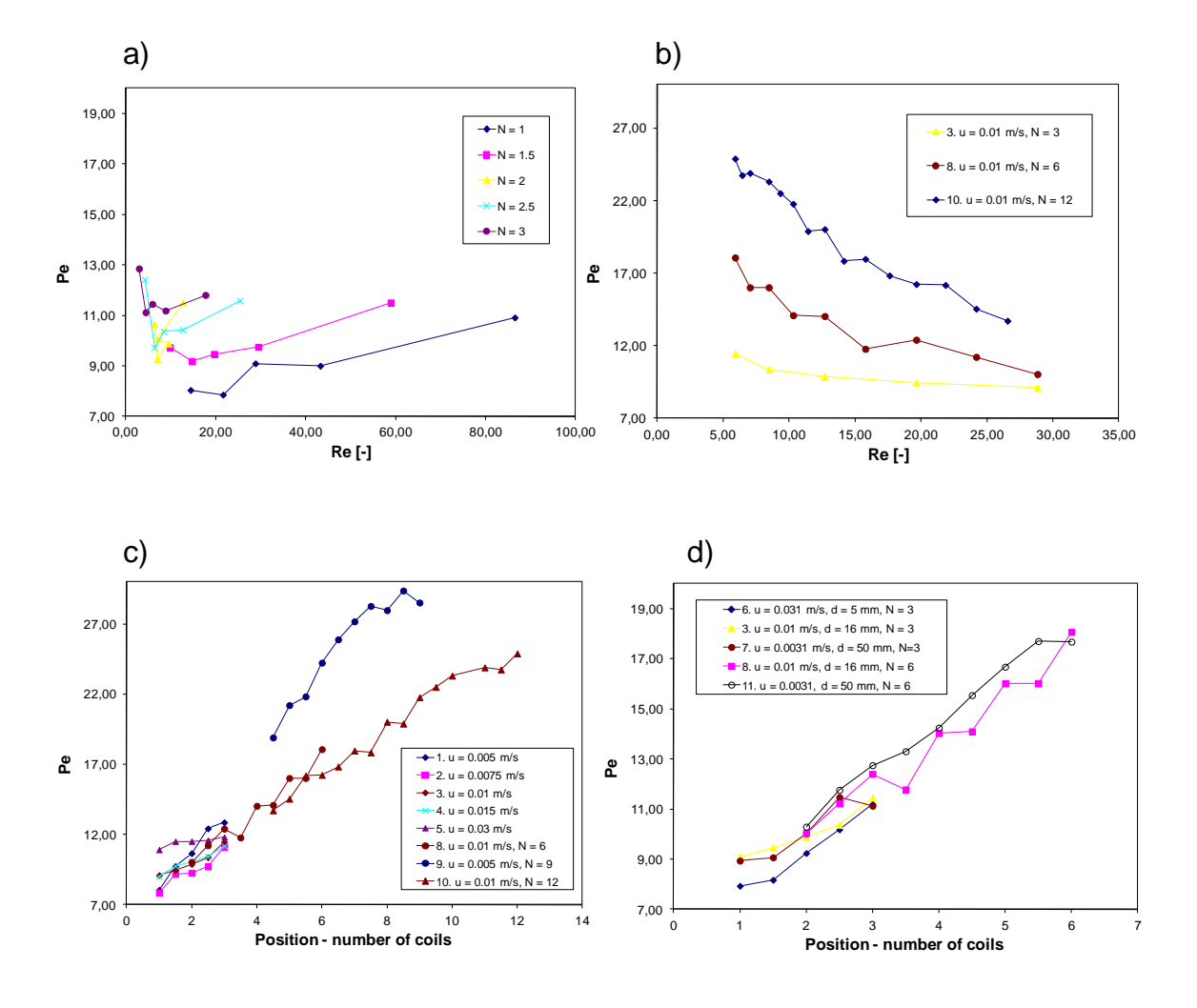
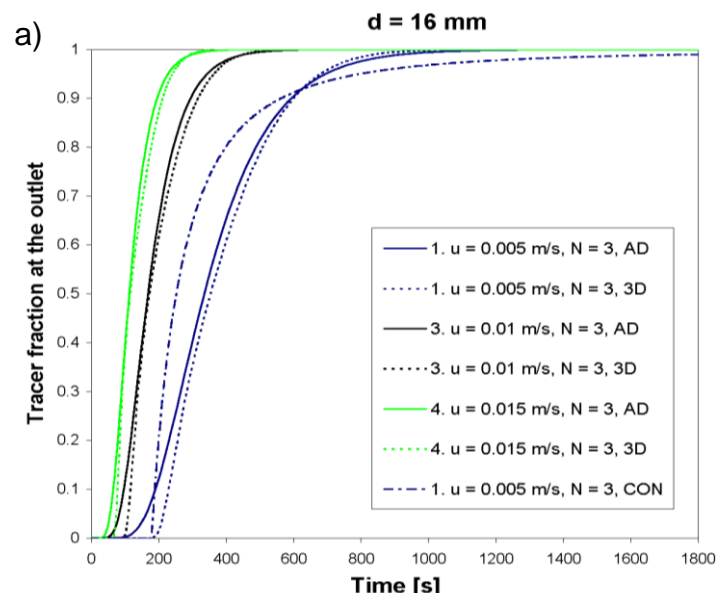
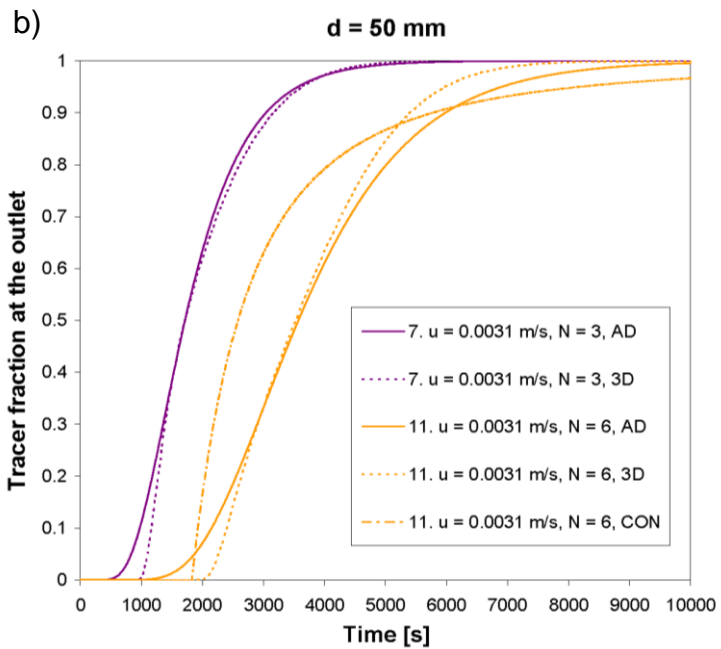


Figure 5. Estimated Pe numbers vs. Re numbers (a and b) and vs. position along the Helix (c and d). a) Lines connect different positions in the three-coil reactors. B) Lines connect positions in different reactors - inlet is on the right hand side (same diameter, different number of coils). c) Lines connect positions along the reactor (same diameter, different inlet velocities). d) Lines connect positions along the reactors of different diameter and number of coils.





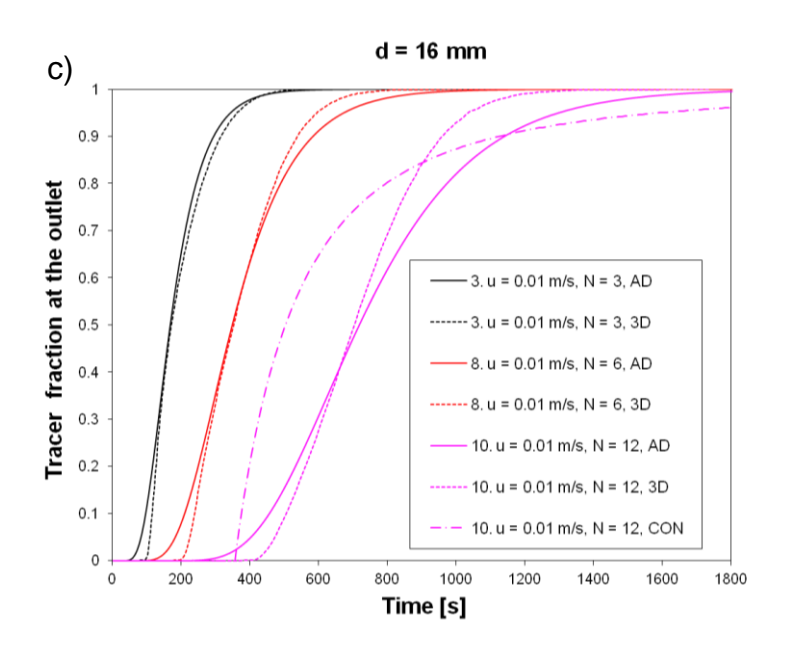


Figure 6. Comparison of F curves obtained from CFD simulations (label 3D), reduced AD model (label AD) and pure convective laminar model (label CON).

a) Same reactor size (diameter and number of coils) and different velocities are used. b) Same reactor diameter (16 mm) and velocity, different number of coils are used. c) Same reactor diameter (50 mm) and velocity, different number of coils are used.